JOURNAL OF CATALYSIS 153, 123–130 (1995)

Sulfated Zirconia Catalysts: Characterization by TGA/DTA/Mass Spectrometry

Ram Srinivasan, Robert A. Keogh, Diane R. Milburn, and Burtron H. Davis

Center for Applied Energy Research, University of Kentucky, 3572 Iron Works Pike, Lexington, Kentucky 40511

Received May 16, 1994; revised November 11, 1994

Sulfated zirconia catalysts, with and without Pt, were subjected to heat treatments in air, helium, or a mixture of hydrogen and helium. Oxygen retards the evolution of the sulfur species while hydrogen accelerates their evolution; thus, the temperature for the evolution of sulfur species is higher in air than in helium and in hydrogen. The loss of sulfur allows the exothermic tetragonal phase transition to monoclinic zirconia to occur. From the temperature of the exotherm and the composition of the evolved gases, it appears that the sulfur species that evolve early in the decomposition contain more oxygen than those that evolve during the later part of the decomposition. Only reduced sulfur species are observed during the heating of Pt–SO_4^{2-}–ZrO_2 in hydrogen; however, reduced species are observed only during the later portion of the decomposition period for the SO_4^{2-}–ZrO_2 sample that does not contain Pt.

INTRODUCTION

Solid oxide catalysts have been widely used in petroleum refineries for skeletal isomerization of *n*-paraffins to isomeric alkanes. The production of oxygenates, which are important components of automobile fuels, may involve chemical reactions such as alkylation, isomerization, and oligomerization, in addition to etherification. These reactions are commonly catalyzed by liquid or solid catalysts.

According to Gillespie's definition (1, 2), a *superacid* is one which exhibits acidity stronger than that of 100% H_2SO_4, i.e., $H_0 \leq -12$. Among a vast number of solid acids, the binary oxides, such as SiO_2–Al_2O_3, TiO_2–ZrO_2, SiO_2–TiO_2, and SiO_2–ZrO_2, exhibit surface acidity stronger than $H_0 = -8.2$ (3–5), and therefore contain few, if any, superacid sites. Since these recently reported superacids have attracted attention for a number of industrial chemical reactions such as isomerization, oligomerization, cracking, and hydrocracking, intense research interest in terms of preparation and characterization was focused on these superacid catalysts. The solid superacids attracted industrial, as well as academic, interest because of their ease of separation from the reaction mixtures. Another advantage of using a solid superacid is that it may decrease or eliminate corrosion of the reactor and the release of corrosive products from the reactor, thus satisfying environmental regulations. However, for many reactions it is the high activity at low temperatures that attracts attention to these catalysts since this permits operation where thermodynamic equilibrium compositions contain a high fraction of the desired isoalkane and/or isoalkene components that have high octane ratings.

Among the solid oxide catalysts, zirconium oxide (ZrO_2) is claimed to be the only oxide catalyst that has acidic, basic, oxidizing, and reducing properties (6). A sulfated zirconia is reported to be a superacid (5, 6). It appears that Holme and Bailey (7) were the first to report the use of such a catalyst. Interest in the sulfated zirconia catalyst intensified in the early 1980s (8–16). In spite of many reports about these catalysts during the past 15 years, the role and nature of the surface acidity and structure of the modified oxides remain elusive. Furthermore, the activation of these catalysts involves complex chemical changes.

Extensive characterization studies have been carried out on sulfate-modified zirconia (17–37), but fewer have been reported for platinum-impregnated sulfated zirconia (38–45). In the present investigation, a simultaneous TGA/DTA/MS technique was utilized to investigate the weight loss and the thermal transformations of the solid and to monitor the chemical compounds that may evolve under controlled heating in different environments. At the same time, the impact of Pt on the transformation was investigated.

EXPERIMENTAL METHODS

Zirconium oxide was prepared by rapidly precipitating from a 0.3 *M* solution prepared from anhydrous $ZrCl_4$ with an excess amount of NH_4OH to a final pH of 10.5 (46, 47). After washing the precipitate thoroughly with water and then with ethanol to remove most of the water, it was dried at 120°C for 2–3 days. The chloride content of the last filtrate was <3 ppm. A slurry containing ZrO_2 powders and 0.5 *M* H_2SO_4 was stirred continuously 2 h

0021-9517/95 $6.00

and then the slurry was filtered (15 ml of 0.5 M H_2SO_4 per gram of catalyst was used for sulfation). The sulfated ZrO_2 powders (SO_4^{2-}–ZrO_2) were dried at 120°C overnight. The chemical analysis showed that this sample contained 3.46% S (10.4 wt% SO_4^{2-}). A portion of the SO_4^{2-}–ZrO_2 sample was impregnated with an aqueous solution of H_2PtCl_6 to attain a concentration of 0.6 wt% platinum in the final catalyst. The Pt-containing sample was dried at 120° overnight (Pt–SO_4^{2-}–ZrO_2).

Differential thermal analysis (DTA), thermogravimetric analysis (TGA), and the mass spectrometry (MS) of the gases evolved from the sulfalted zirconia catalyst were simultaneously conducted using a Seiko TG/DTA 320 instrument which was coupled to a VG Micromass quadrupole mass spectrometer. This Seiko instrument has an operating range from room temperature to 1200°C. The runs were conducted separately in a purge gas of helium, air, or a H_2/He mixture. For the runs conducted in helium or in air, a flow rate of 200 ml/min was used; the H_2/He mixture consisted of 100 ml/min H_2 and 200 ml/min He. Heating rates were 20°C/min except for the few runs at 10°C/min. Platinum crucibles were used as sample holders and Al_2O_3 was used as a reference material. The TGA unit was connected to a disk station that allows for the performance of programmable heating and cooling cycles, continuous weight measurements, sweep gas valve switching, and data analysis.

A VG Instruments SXP600 quadrupole mass spectrometer (MS) was used to conduct "evolved gas analysis" (EGA) concurrently with the DTA/TG runs. This mass spectrometer allows the determination of multiple gas components in the mass range of 1–300 amu. The mass spectrometer was interfaced to the DTA/TG unit by a fused silica capillary transfer line inserted just above the sample in the chamber of the DTA unit. To prevent condensation inside the capillary, it was maintained at 170°C by self-resistance heating. The flow rate through the capillary was about 12 ml/min at 170°C. The mass spectrometer has a Vier-type enclosed ion source, a triple mass filter, and two detectors (a Faraday cup and a secondary emission multiplier). Data from the mass spectrometer was acquired using a log histogram mode (LHG) in which the intensities of all peaks in a specified mass range (e.g., 1–100 amu) were monitored and stored repeatedly during the temperature program. A data conversion program was then used to display the intensities of the desired ions as a function of time. In this manner the changes in the concentration of a species in the gas stream can be followed and related through the time scale to the DTA and TG events.

RESULTS

The total weight loss curves resulting from heating the SO_4^{2-}–ZrO_2 sample in air, helium, or a H_2/He mixture are presented in Fig. 1. The total weight loss was about 18% for this sample in each of the three environments. The unsulfated ZrO_2 showed a total weight loss of only about 12% when heated under the same conditions (46). Two major weight loss regions are identified for the SO_4^{2-}–ZrO_2 sample. The first major weight loss of about 10–12% is observed between 100–500°C and the second weight loss of about 6–8% is observed above 500°C. This result was the same whether the sample was heated in air, helium, or a H_2/He mixture.

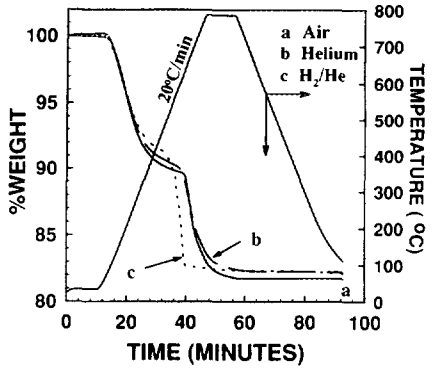

FIG. 1. Weight loss curves plotted as percent initial weight against time (min) for the sample SO_4^{2-}–ZrO_2 heated: (a) in air, (b) in helium, and (c) in a H_2/He mixture. Also shown in this figure is the temperature–time profile.

The DTA data were collected simultaneously with the TGA and MS data. The three curves shown in Fig. 2 correspond to the scans in air (a), helium (b), and a H_2/He mixture (c). An exotherm occurs at 614°C when the sample is heated in helium and at 622°C when it is heated in air. The exotherm corresponds to the transformation of zirconia from a material that is amorphous to X-ray diffraction to the tetragonal phase and corresponds to a loss of surface area as well (48, 49). This exotherm occurs at about 450°C for zirconia, but is shifted to a higher temperature when sulfate is present. Depending

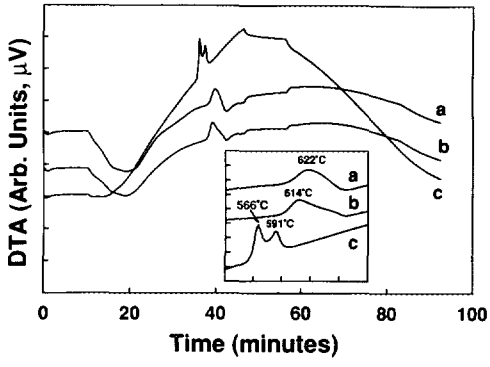

FIG. 2. The DTA curves for the SO_4^{2-}–ZrO_2 sample heated: (a) in air, (b) in helium, and (c) in a H_2/He mixture.

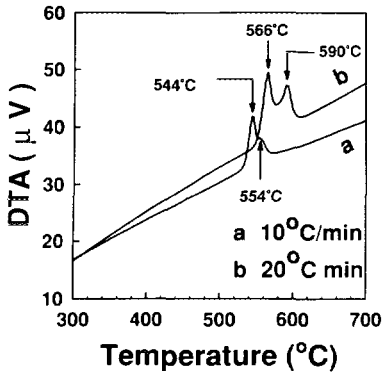

FIG. 3. The DTA curves for heating the SO_4^{2-}–ZrO_2 the sample in a H_2/He mixture at two heating rates: (a) 10°C/min, and (b) 20°C/min.

upon the sample, the heating rate, etc., the exothermic crystallization may occur before the endothermic decomposition of the sulfate has been completed. Thus, the exothermic event for heating the sample in air or an inert gas is the result of an exothermic and an endothermic event so that the shape of the trace will depend upon the heat balance for these two events.

The presence of hydrogen causes the exothermic processes to occur at a lower temperature, and two distinct exothermic peaks are obtained. The first exotherm that appears is centered at about 566°C and the second at 591°C. The rate of heating influences the position of the doublet (Fig. 3). The exotherm data in the H_2/He mixture are presented for two heating rates: 10 and 20°C/min. A part of the differences between the two heating rate curves are likely to be a result of slight differences between the temperature of the sample and the indicating thermocouple. The exothermic doublet peaks are very clear for the heating rate of 20°C/min. An exothermic peak is obtained when unsulfated zirconia is heated and this corresponds to sintering to a lower surface area material (48). This sintering is responsible for the exothermic peak when heated in air or helium, and, as shown later, for the first peak when heated in a H_2/He mixture. The second exothermic event for the sample heated in hydrogen is a result of reduction of the oxides of sulfur to produce H_2S and H_2O, as shown by the MS data described below.

The MS data obtained for the SO_4^{2-}–ZrO_2 are presented in Fig. 4. When heated in helium, this sample evolved gases with prominent peaks corresponding to the masses: (a) 16 (O), (b) 18 (H_2O), (c) 32 (O_2/S), (d) 44 (CO_2), (e) 48 (SO), and (f) 64 (SO_2). As can be seen in Fig. 4, the first weight loss corresponds to the evolution of water (mass 18) and the second weight loss can be attributed to the evolution of gases that produce peaks of 16, 32, 48, and 64 mass numbers. Mass spectroscopy intensities corresponding to the evolution of H_2S (mass 34) and SO_3 (mass 80) were not observed. The intensity of the H_2S (mass 34) peak, if present, was low and a small amount of H_2S may have evolved prior to the exotherm but not in the region of the exotherm. The CO_2 trace shown in Fig. 4 is due to ethanol which was used as a final wash solvent in the preparation of some of the samples. Thus, the major gaseous species evolved during the period of the exotherm at 610–720°C is SO_2; however, SO_3, if evolved, most likely would not be detected because it could decompose following evolution, as well as in the MS chamber, to produce SO/SO_2 and oxygen. When this sample was heated in air, the same results were obtained as those for the sample run in helium, except for the temperature of the exotherm. The results obtained for various portions of the samples are reproducible.

For clarity, in this and other figures, one trace is shown for peaks of masses 16 and 32; the actual intensities for the two masses are not the same but the two traces have an identical shape.

The MS data obtained for SO_4^{2-}–ZrO_2 heated in H_2/He are shown in Fig. 5. In this gas flow, two major weight losses were observed. The first weight loss was primarily due to water loss. However, the second weight loss was due to the evolution of sulfur in both oxidized (SO_x) and reduced (H_2S) forms. Mass spectroscopy peaks corresponding to the evolution of SO_2 (we write SO_2 even though we realize it may be evolved as SO, SO_2, and/or SO_3) which were observed in helium or in air were also observed in a hydrogen atmosphere. However, the oxides of sulfur are released predominantly (or only) in the tem-

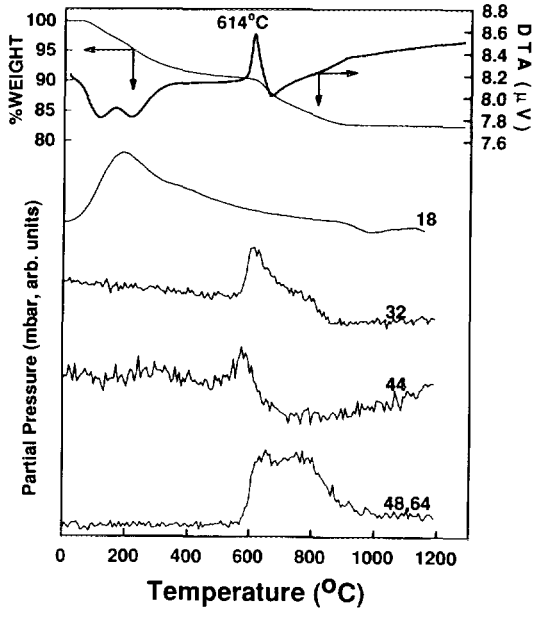

FIG. 4. The evolution of gases of various masses with respect to time (and temperature) and corresponding weight losses when SO_4^{2-}–ZrO_2 was heated in helium.

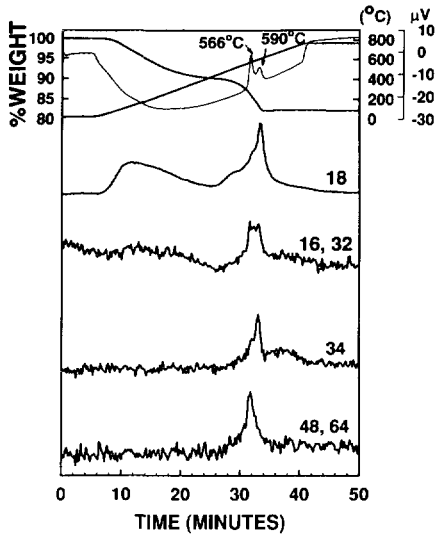

FIG. 5. The mass spectrometric data for the sample SO_4^{2-}–ZrO_2 when heated in a H_2/He mixture showing that the first weight loss corresponds to water loss and the second weight loss corresponds to H_2O, SO_2, H_2S, and O_2 loss.

perature region corresponding to the region of the first exotherm peak (Fig. 5). The second exotherm appears to be due to the exothermic reaction between hydrogen and the oxides of sulfur. Thus, the predominant gas species detected in the region of the second exothermic peak are H_2S and H_2O.

In summary, the SO_4^{2-}–ZrO_2 catalyst that does not contain platinum exhibited two major weight loss regions during heating at a constant rate to 800°C. The first major weight loss was due to the evolution of water and the second major weight loss (above 500°C) was attributed to the evolution of the oxides of sulfur when the sample was run in either helium or air. When the sample is heated in H_2/He, there are two high temperature exothermic regions, and both of these exotherms occur at a lower temperature than when the sample is heated in helium or air. The gases evolved during the first exothermic event are essentially the same as those evolved when the sample is heated in air (oxides of sulfur). The second exothermic event corresponds to the evolution of H_2S and H_2O, which can be attributed to the reduction of sulfur oxides by hydrogen.

The weight loss curves obtained for Pt–SO_4^{2-}–ZrO_2 during heating to 800°C in air, helium, or in the H_2/He mixture are presented in Fig. 6. For these samples two distinct weight loss regions are observed. The first weight loss was due to the evolution of water.

The DTA data obtained for the Pt–SO_4^{2-}–ZrO_2 catalyst in air, helium, and an H_2/He mixture are shown in Fig. 7. In helium, this sample exhibited an exotherm at 574°C but in air the exotherm was very broad and centered at

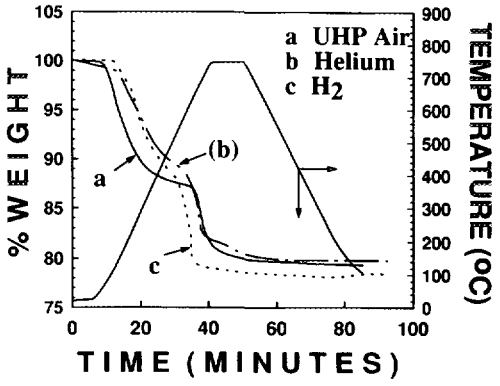

FIG. 6. Weight loss curves plotted as percent initial weight against time (min) for the Pt–SO_4^{2-}–ZrO_2 sample when heated: (a) in air, (b) in helium, and (c) in a H_2/He mixture.

665°C. The exotherm at 528°C in the H_2/He mixture was sharp and was not a doublet. The DTA scans for two heating rates (Fig. 8) show a shift in the exotherm and suggest that there is a temperature difference between the indicating thermocouple and the sample. The shift could also be due to the variety of reactions, the differences in the rate parameters (E_a and A), and the fact that the decompositions are not instantaneous. The exotherm for Pt–SO_4^{2-}–ZrO_2 was not a doublet as was observed for the sulfated ZrO_2 that did not contain platinum. The presence of platinum causes the doublet for the SO_4^{2-}–ZrO_2 sample to appear as a single peak. The presence of platinum and hydrogen causes the exotherm to occur at a lower temperature (528°C).

The mass spectrometric data for the Pt–SO_4^{2-}–ZrO_2 sample heated in air are presented in Fig. 9, along with the corresponding weight loss curve. The masses for SO (mass 48) and SO_2 (mass 64) were obtained during the second weight loss while only the mass for water 18 evolved within the first major weight loss region; because

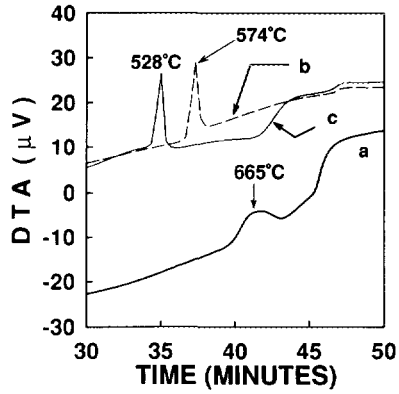

FIG. 7. The DTA curves for the Pt–SO_4^{2-}–ZrO_2 sample heated: (a) in air, (b) in helium, and (c) in a H_2/He mixture.

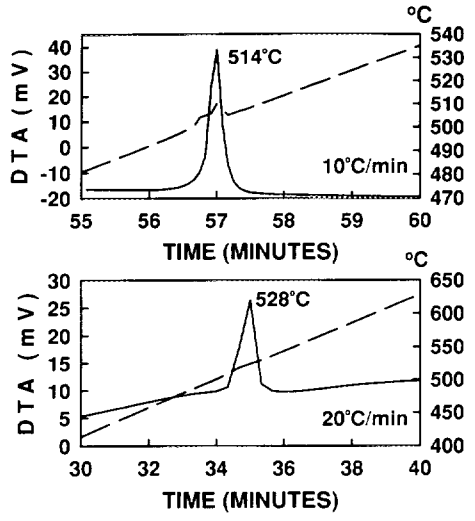

FIG. 8. The DTA curves for the Pt–SO_4^{2-}–ZrO_2 sample run in a H_2/He mixture at (a) 10°C/min and (b) 20°C/min heating rates.

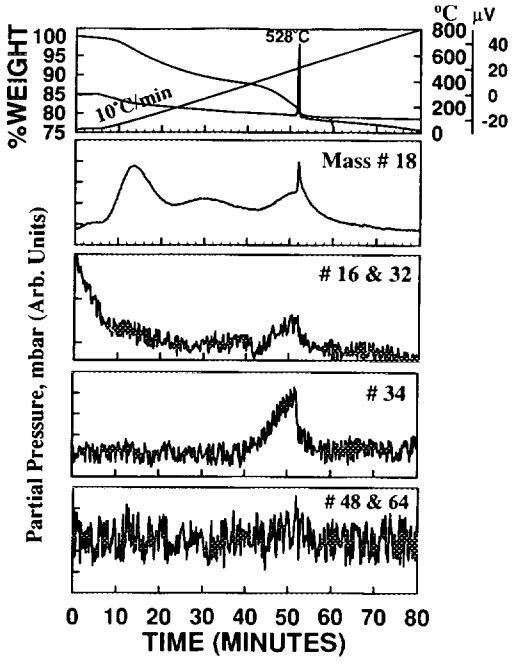

FIG. 10. Masses of the gases evolved during heating Pt–SO_4^{2-}–ZrO_2 in a H_2/He mixture.

air was added, mass 32 is not shown. During the first weight loss a small amount of H_2S (mass 34) may have evolved, but the intensity of this mass was, at most, barely above the background noise. Similar observations were made for the run in helium, except that in this instance, oxygen (mass 32) was also observed. When the Pt–SO_4^{2-}–ZrO_2 sample was heated in the H_2/He mixture, gases evolved with mass of 16, 18, 32, and 34 corresponding to H_2O and H_2S (Fig. 10). Peaks corresponding to SO or SO_2 were not observed. Thus, with hydrogen present, the SO_2 and/or SO_3 that evolved were rapidly hydrogenated to produce water and H_2S or the SO_x species was hydrogenated prior to desorption. The amount of water formed during the higher temperature weight loss region was greater when Pt was present.

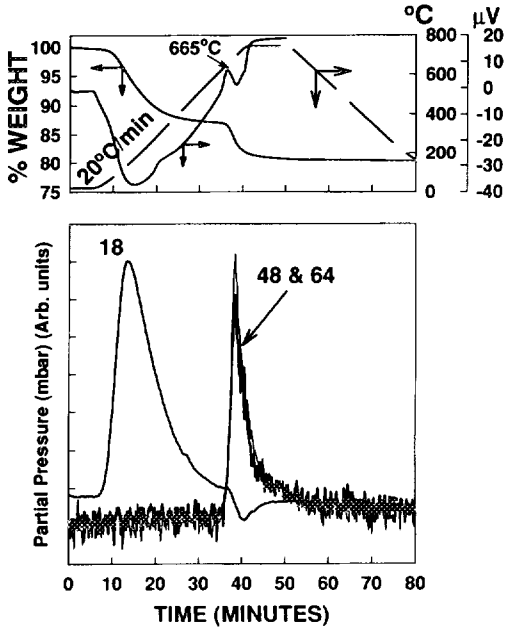

FIG. 9. Masses of the gases evolved during heating Pt–SO_4^{2-}–ZrO_2 sample in air.

Attempts were made to simulate the heating/cooling conditions that were used for the reaction studies with the Pt–SO_4^{2-}–ZrO_2 sample. This catalyst was used for hexadecane conversion, following activation at 725°C for 2 h and then cooling to room temperature in a dessicator. A catalyst which was activated in a muffle furnace at 725°C for 2 h was mounted into the TGA unit. This sample was then heated at a controlled rate (20°C/min) to 800°C in helium. On heating no significant weight losses were observed for this prior-activated sample, nor was it possible to observe the evolution of any gas. This was also the case when a similar sample of the prior-activated material was heated in a H_2/He mixture. This clearly indicates that the associated weight losses and mass evolution are one time occurrences and these events occur only on the first heating of the fresh catalysts. These results were reproducible during six runs for each of the prior-activated samples.

The results of chemical analyses for several samples that have been heated at 725°C in air or inert gas show that the sulfur content is about 1 ± 0.3 wt%. Samples

heated in hydrogen under conditions such as those used in this study contain about 0.6 ± 0.2 wt% sulfur.

DISCUSSION

The TGA results indicate that there is a total weight loss of about 12% for the unsulfated zirconia, and of about 18% for SO_4^{2-}–ZrO_2 and Pt–SO_4^{2-}–ZrO_2. The curves for both SO_4^{2-}–ZrO_2 and Pt–SO_4^{2-}–ZrO_2 catalysts exhibit two distinct weight loss regions. The first weight loss of about 8–12% occurs during heating to 550°C, and this corresponds to water loss as evidenced by both the endothermic DTA peak and the appearance of the mass 18 (H_2O) peak. The variation in the weight loss in this region depends upon the drying conditions and the amount of SO_4^{2-} added by soaking in H_2SO_4. The second weight loss of about 6–8% occurs beyond 550°C, and this corresponds to the evolution of different species in different environments.

The products evolved in the temperature region above 500°C show that there is a burst of oxygen (mass 32) that coincides with the evolution of sulfur oxides; however, the amount of oxygen reaches a maximum and then declines to near to the baseline value more rapidly than the peaks corresponding to SO_2/SO. Since it is unlikely that most, if any, of the O_2 is liberated directly from the solid, this suggests that SO_3 is evolved to a greater extent during the early period of the evolution of sulfur oxides than during the later periods. Thus, in the inert gas the heating events can be described as occurring in two temperature regions, with the second region being further divided into at least two subdivisions:

Region I (<500°C)

$$(SO_4^{2-}\text{–}ZrO_2(OH)_2 \cdot (H_2O)_x \rightarrow (SO_4^{2-})\text{–}ZrO_2 + (x+1)\,H_2O \quad [1]$$

Region II (>500°C) Subdivision I (lower temperature region)

$$SO_4^{2-}\text{–}ZrO_2 \rightarrow ZrO_2(O_a) + SO_3 \quad [2]$$

$$SO_3 \rightarrow SO_2\,(\text{or SO}) + O\,(\text{or } O_2) \quad [3]$$

Region II (>500°C) Subdivision II (higher temperature region)

$$SO_4^{2-}\text{–}ZrO_2 \rightarrow ZrO_2 + SO_2\,(\text{or SO}) + xO_a + yO_2 \quad [4]$$

in the above equations, it is realized that some or all of the SO_4^{2-} is likely to be present in the solid in a variety of structures such as:

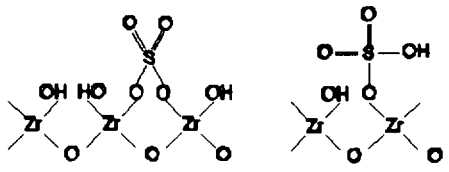

[5]

However, we have written the structure of the sulfated gel as SO_4^{2-}–$ZrO(OH)_2$ since the extent to which the structures in [5], or similar structures, are present in the dried gel is not known. Likewise, it is realized that the material present at the end of the first heating region cannot be SO_4^{2-}–ZrO_2, and that the actual structure likely contains less oxygen than shown by this structure. Likewise, the decomposition of SO_4^{2-}–ZrO_2 requires that adsorbed oxygen be formed, and for illustration this is shown as O_a. However, these equations illustrate the general observation that the sulfur species that evolve to the gas phase contain less oxygen as the decomposition progresses. The results obtained when the pretreating gas was air are similar to those of the run in helium; however, when air is used it is not possible to measure the evolution of oxygen.

The mass spectrometry data provide an explanation for the two exotherm peaks that are observed when SO_4^{2-}–ZrO_2 is heated in the H_2/He mixture. During the first exotherm (Fig. 5), the liberation of sulfur oxides are documented by the presence of the peaks corresponding to masses of 48 (SO) and 64 (SO_2); also masses of 16 (O) and 32 (O_2 and possibly S) are observed. During the period of the second exotherm little, if any, sulfur oxides are observed as products; rather peaks with masses of 18 (H_2O) and 34 (H_2S) are obtained. Thus, it appears that the weight loss associated with the region of the first exotherm is due to the loss of SO_3 as was based on the observations when this sample was heated in helium or air. As the SO_3 is lost, the tetragonal phase of zirconia becomes unstable and the zirconia transforms to the monoclinic phase with the evolution of heat that is exhibited by the first exotherm (see Fig. 2; 566°C when heated at 20°/min.). It has been demonstrated that sulfate stabilizes both the tetragonal phase and a high surface area during calcination of the sample (19, 46, 50). Thus, the first exotherm is due to the occurrence of reactions [2] and [3] and the loss of surface area. The second exotherm is due to the reduction of sulfur oxides to produce H_2S and H_2O. The gas flow over the sample is too fast for the second exotherm to be due to the reduction of the SO_3 that is evolved during the first exotherm; the evolved SO_3 would be swept from the sample zone prior to the period of the second exotherm. Thus, we conclude that the zirconia is not a catalyst for the reduction of the sulfur oxides until a significant portion of the surface has been exposed by the loss of sulfur oxides. The second exotherm therefore is postulated to correspond to the Region II, subdivision

TABLE 1

Exotherm Temperature for SO_4^{2-}–ZrO_2 and Pt–SO_4^{2-}–ZrO_2 Heated in Various Pretreatment Gases

Pretreatment gas	Exotherm temperature (C)	
	SO_4^{2-}–ZrO_2	Pt–SO_4^{2-}–ZrO_2
Air	622	665
Helium	614	574
Hydrogen/helium	575	528

II reactions (Eqs. [6] and [7]). These reactions occur when sufficient zirconia surface is free of sulfur oxides so that the reduction of sulfur oxide can occur; thus, in a flow of hydrogen we have to modify the reactions that occur:

Region II, Subdivision II (H_2)

$$SO_4^{2-}\text{–}ZrO \rightarrow ZrO_2(O_a) + SO_2 \text{ (or SO)} \quad [6]$$

$$H_2 + SO_2 \text{ (or SO)} \rightarrow H_2S + 2H_2O \text{ (or } H_2S + H_2O) \quad [7a]$$

$$O_a + H_2 \rightarrow H_2O. \quad [7b]$$

The reactions represented by Eqs. [7a] and [7b] are exothermic and therefore are responsible for the second exotherm.

It appears that the presence of Pt alters the evolution of sulfur oxides. In a flow of air the decomposition to evolve sulfur oxides occurs during a similar time period (4–5 min) but at a higher temperature when Pt is present (665 vs. 622°C, Table 1). However, when the Pt–SO_4^{2-}–ZrO_2 sample is heated in helium, it appears that the evolution of sulfur oxides occurs at a lower temperature (574 vs. 614°C, Table 1) and the decomposition occurs more rapidly in helium (1.5 min) than in air (~4 min). However, additional studies with samples that contain various levels of sulfur would have to be utilized to confirm these apparent differences.

The presence of both hydrogen and Pt alters the course of sulfur evolution. Just as in the case for the SO_4^{2-}–ZrO_2 sample, the evolution of sulfur occurs at a lower temperature in the presence of hydrogen. Furthermore, the evolution of the sulfur species occurs for about 1.5 min when Pt is present rather than for about 3.5 min in the absence of Pt. In addition, the reduction of the oxides of sulfur is rapidly catalyzed by Pt so that only the reduced form of sulfur, H_2S, is observed; sulfur oxides, if present, are at such a low concentrations that they cannot be detected. Thus, the exothermic reduction of the sulfur oxides occur in the same temperature region as that of the tetragonal to monoclinic phase transformation.

It appears that the presence of oxygen (air flow) retards the evolution of sulfur species from both SO_4^{2-}–ZrO_2 and Pt–SO_4^{2-}–ZrO_2, with the retardation being greater for SO_4^{2-}–ZrO_2, than when the decomposition occurs in an inert gas, helium (Table 1). In addition to the higher temperature for elimination, it appears that the loss of sulfur species is more rapid in the inert gas than in the presence of oxygen, especially for Pt–SO_4^{2-}–ZrO_2. For the Pt–SO_4^{2-}–ZrO_2 catalyst it appears that the sulfur species are evolved over a similar time period. However, the lower temperatures for the decomposition of SO_4^{2-}–ZrO_2 (575°C) and Pt–SO_4^{2-}–ZrO_2 (528°C) suggest that hydrogen reacts with the sulfur oxides while they are present in and/or on the solid phase rather than after they desorb to the gas phase. Furthermore, the lower temperature for the loss of sulfur when Pt is present suggests that hydrogen spillover (or some other activation mechanism) occurs.

REFERENCES

1. Gillespie, R. J., *Acc. Chem. Res.* **1,** 202 (1968).
2. Gillespie, R. J., and Peel, T. E., *Adv. Phys. Org. Chem.* **9,** 1 (1972).
3. Tanabe, K., "Solid Acids and Basis, Their Catalytic Properties," Tokyo Kodansha, Academic Press, New York, 1970.
4. Tanabe, K., *in* "Catalysis—Science and Technology" (J. R. Anderson and M. Boudart, Eds.), Vol. 2, Springer-Verlag, Berlin, 1981.
5. Tanabe, K., *in* "Proceedings, 9th International Congress on Catalysis, Calgary, 1988" (M. J. Phillips and M. Ternan, Eds.), Chem. Institute of Canada, Ottawa, 1988.
6. Tanabe, K., *Mater. Chem. Phys.* **13,** 3479 (1985).
7. Holme, V. C. F., and Bailey, G. C., U. S. Patent 3, 032, 599 (1962).
8. Hino, M., and Arata, K., *Chem. Commun.*, 851 (1980).
9. Jin, T., Machida, M., and Tanabe, K., *Inorg. Chem.* **23,** 4396 (1984).
10. Yamaguchi, T., Jin, T., and Tanabe, K., *J. Phys. Chem.* **90,** 3148 (1986).
11. Jin, T., Yamaguchi, T., and Tanabe, K., *J. Phys. Chem.* **90,** 4794 (1986).
12. Yamaguchi, T., Jin, T., Ishida, T., and Tanabe, K., *Mater. Chem. Phys.* **17,** 3 (1987).
13. Matsuhashi, H., Hino, M., and Arata, K., *Chem. Lett.*, 1027 (1988).
14. Hino, M., and Arata, K., *J. Chem. Soc. Chem. Commun.*, 1259 (1987).
15. Ishida, T., Yamaguchi, T., and Tanabe, K., *Chem. Lett.*, 1869 (1988).
16. Tanabe, K., *Crit. Rev. Surf. Chem.* **1,** 1 (1990).
17. Srinivasan, R., and Davis, B. H., Preprint, Division of Petroleum Chemistry, Am. Chem. Soc., 203rd National Meeting, New York **36,** 4, 635 (1991).
18. Srinivasan, R., and Davis, B. H., *Catal. Lett.* **14,** 165 (1992).
19. Srinivasan, R., Taulbee, D., and Davis, B. H., *Catal. Lett.* **9,** 1 (1991).
20. Srinivasan, R., Cavin, O. B., Hubbard, C. R., and Davis, B. H., *J. Am. Ceram. Soc.* **75,** 1217 (1992).
21. Davis, B. H., Keogh, R., and Srinivasan, R., *Catal. Today* **20,** 219 (1994).
22. Arata, K., "Advances in Catalysis," Vol. 37, pp. 165–211. Academic Press, 1990.
23. Morterra, C., Cerrato, G., Emanuel, C., and Bolis, V., *J. Catal.* **142,** 349 (1993).
24. Yamaguchi, T., and Tanabe, K., *Mater. Chem. Phys.* **16,** 67 (1986).
25. Bensitel, M., Saur, O., Lavalley, J. C., and Mabilon, G., *Mater. Chem. Phys.* **17,** 249 (1987).
26. Scurrell, M. S., *Appl. Catal.* **34,** 109 (1987).

27. Chen, F. R., Coudurier, G., and Joly, J. F., Division of Petroleum Chemistry, 203rd Am. Chem. Soc. National Meeting, New York, 1991.
28. Yamaguchi, T., *Appl. Catal.* **61,** 1 (1990).
29. Xu, B. Q., Yamaguchi, T., and Tanabe, K., *Appl. Catal.* **64,** 41 (1990).
30. Tanabe, K., "Critical Reviews in Surface Chemistry," Vol. I, pp. 1–25. CRC Press, Boca Raton, FL, 1990.
31. Tanabe, K., *Mater. Chem. Phys.* **13,** 347 (1985).
32. Mukaida, K., Miyoshi, T., and Satoh, T., *in* "Acid–Base Catalysis" (K. Tanabe, *et al.*, Eds.), p. 363. Kodansha, Tokyo, 1989.
33. Arata, K., Hino, M., and Yamagata, N., *Bull. Chem. Soc. Jpn.* **63,** 244 (1990).
34. Tanaka, T., Itagaki, A., Zhang, G., Hattori, H., and Tanabe, K., *J. Catal.* **122,** 384 (1990).
35. Xu, B., Yamaguchi, T., and Tanabe, K., *Chem. Lett., Chem. Soc. Jpn.*, 1663 (1988).
36. Hino, M., Kobayashi, S., and Arata, K., *J. Am. Chem. Soc.* **101**(21), 6439 (1979).
37. Bolis, V., Morterra, C., Volante, M., Orio, L., and Fubini B., *Langmuir* **6,** 695 (1990).
38. Wen, M. Y., Wender, I., and Tierney, J. W., *Energy Fuels* **4,** 372 (1990).
39. Evitani, K., Tanaka, T., and Hattori, H., *Appl. Catal. A* **102,** 79 (1993).
40. Hosoi, T., Shimadzu, T., Ito, S., Baba, S., Takaoka, H., Imai, T., and Yokoyama, N., *Prepr. Symp. Div. Petr. Chem. Am. Chem. Soc.*, 562 (1988).
41. Ebitani, K., Kouishi, J., and Hattori, H., *J. Catal.* **130,** 257 (1991).
42. Iglesia, E., Soled, S. L., and Kramer, G., *J. Catal.* **144,** 238 (1993).
43. Paal, Z., Muhler, M., and Schlogl, R., *J. Catal.* **143,** 318 (1993).
44. Ebitani, K., Tanaka, K. H., and Hattori, H., *J. Catal.* **135,** 60 (1992).
45. Ebitani, K., Konno, H., Tanaka, T., and Hattori, H., *J. Catal.* **143,** 322 (1993).
46. Chokkaram, S., Srinivasan, R., Milburn, D. R., and Davis, B. H., *J. Colloid Interface Sci.* **165,** 160 (1994).
47. Srinivasan, R., Harris, M. B., Simpson, S. F., De Angelis, R. J., and Davis, B. H., *J. Mater. Res.* **3,** 787 (1988).
48. Srinivasan, R., and Davis, B. H., *J. Colloid Interface Sci.*, **156,** 400 (1993).
49. Srinivasan, R., Cavin, O. B., and Hubbard, C. R., *Chem. Mater.* **5,** 27 (1993).
50. Chen, F. R., Coudurier, G., Joly, J. F., and Vedrine, J. C., *J. Catal.* **143,** 616 (1993).